Jurnal
Teknologi

Full Paper

NUMERICAL STUDY ON THE EFFECT OF DIFFERENT VISCOMETER TEST ON STENCIL PRINTING PROCESS

M. H. H. Ishak[a], M. S. Rusdi[b*], M. Z. Abdullah[b], M. S. Abdul Aziz[b], M. K. Abdullah[c], P. Rethinasamy[d], Damian G. Santhanasamy[e]

[a]School of Aerospace Engineering, Engineering Campus, Universiti Sains Malaysia, 14300 Nibong Tebal, Penang, Malaysia
[b]School of Mechanical Engineering, Engineering Campus, Universiti Sains Malaysia, 14300 Nibong Tebal, Penang, Malaysia
[c]School of Materials and Mineral Resources Engineering, Engineering Campus, Universiti Sains Malaysia, 14300 Nibong Tebal, Penang, Malaysia
[d]Celestica Malaysia Sdn. Bhd., Plot 15, Jalan Hi-Tech 2/3 Phase I, Kulim Hi-Tech Park,09000 Kulim, Malaysia
[e]Indium Corporation of America, 29 Kian Teck Avenue, Singapore 628908

Article history
Received
16 November 2021
Received in revised form
15 June 2022
Accepted
25 July 2022
Published Online
31 October 2022

*Corresponding author
syakirin@usm.my

Graphical abstract

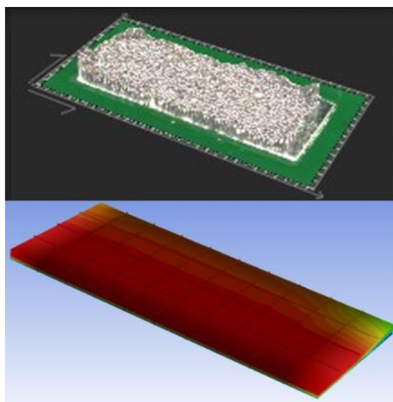

Abstract

Using CFD simulation, this study analyses the applicability of several spindle types for assessing lead-free solder paste. The purpose of this investigation is to determine how much solder paste applied on the solder pad. Five separate studies were conducted on parallel-plate (PP) and cone-plate (CP) spindles. The simulation was performed by using the Volume of Fluid (VOF) approach, and the Cross model represented solder paste viscosity. Since it is popularly used in modern industry, lead-free solder paste SAC305 type 3 was chosen for this study. Regardless of squeegee speed or aperture size, solder paste always filled the volume. The PP with 0.5 mm gap exhibits the smallest average disparity between simulation and experiment for all squeegee speeds tested. For 1° CP, all experiments show similar trend line with average disparity except for 0.5 mm PP. All tests with very small aperture volumes produced comparable filled volume values, except for 0.5 mm PP test, which showed the smallest percentage change when the experimental data is compared at higher aperture volumes. This method can be used by other simulation researchers to get solder paste's viscosity data for their solder paste simulation.

Keywords: SAC305, lead-free solder paste, Stencil Printing, Viscometer, SMT Simulation

Abstrak

Simulasi Perkomputeran Dinamik Bendalir (CFD) digunakan untuk kajian ini bagi membincangkan penggunaan jenis gelendung yang berbeza untuk ujian pes pateri bebas plumbum. Kajian ini dijalankan untuk mengukur isipadu pemendapan tampal pateri pada pad pateri. Gelendong plat selari (PP) dan plat kon (CP) telah digunakan bagi Menkalinan lima ujian yang terdiri daripada jenis dan tetapan gelendong yang berbeza. Kaedah Isipadu Cecair (VOF) digunakan untuk simulasi manakala model Cross digunakan sebagai model kelikatan untuk pes pateri. Pes pateri tanpa plumbum SAC305 Jenis 3 telah digunakan dalam kajian ini kerana ia

merupakan pes pateri yang paling popular digunakan oleh industri pada masa kini. Pes pateri sentiasa mengisi isi padu pateri sepenuhnya tanpa mengira kelajuan sapuan dan saiz pembukaan yang digunakan. Untuk setiap kelajuan sapuan yang diuji, PP dengan jurang sebanyak 0.5 mm sentiasa memperolehi nilai sisihan purata terendah apabila dibandingkan di antara simulasi dan eksperimen. Untuk 1º CP, kesemua ujian telah menunjukkan garis arah aliran yang serupa di antara satu sama lain beserta nilai sisihan purata yang sama kecuali 0.5 mm PP. Kesemua ujian menggunakan isi padu pembukaan yang kecil telah menunjukkan nilai isi padu terisi yang setanding di antara satu sama lain kecuali 0.5 mm PP yang memperolehi nilai perbezaan peratusan terendah apabila data-data eksperimen dibandingkan apabila menggunakan isi padu pembukaan yang lebih besar. Kaedah ini bersesuaian untuk digunakan oleh penyelidik simulasi lain untuk medapatkan data berkenaan kelikatan pes pateri untuk kegunaan simulasi pes pateri mereka.

Kata kunci: SAC305, Pes pateri tanpa plumbum, Cetakan stensil, Viscometer, Simulasi SMT

© 2022 Penerbit UTM Press. All rights reserved

1.0 INTRODUCTION

Electronic items are continuously innovating and becoming more complex as time passes; concurrently, they are becoming more intelligent and more compact [1]. This breakthrough should be supported by improvements in manufacturing of electronic component. Electronic boards are manufactured using Surface Mount Technology (SMT) in electronics sector. The method consists of numerous processes, which involves a bare Printed Circuit Board (PCB) at the start and finished with a PCB that has been filled with electrical components.

The procedure starts off using method of stencil printing as the first phase. This method revolving around depositing solder paste on a solder pad while using stencil to guide its placement. This approach, which can be seen in Figure 1, made use of a squeegee that operated at an angle which guarantee the solder paste to perfectly swept into the designated opening area. This approach is responsible for approximately 60% of all faults and failures exhibit by products manufactured by using SMT [2, 3]. After making the move to lead-free solder paste and soldering reduction in pad and component, the defects observed were much more substantial than they had been previously [4]. There have been a few different attempts made to experiment with stencil printing [5, 6, 7], and overall expenditures of creating and testing stencil printing systems experimentally often include both monetary and time commitments. Alternatively, the characterisation of solder paste stencil printing process may also be investigated through the use of numerical simulations, such as computational fluid dynamics (CFD), which give an in-depth study and sample set of valuable findings.

Krammer [8] used the Finite Volume Method (FVM) to conduct a study in which he contrasted simulations of solder paste that were based on Newtonian and non-Newtonian models. Based on the findings, one can deduce that a non-Newtonian model should be utilised in order to accurately simulate the behaviour of solder paste. Inaccuracies in the calculations will occur if the real material qualities of the solder paste are not taken into consideration. In addition, Durairaj *et al.*, (2002) used a computational fluid dynamics (CFD) technique to investigate the relationship between altering the speed of the squeegee and increasing the amount of solder paste [9]. They did this by analysing the relationship between the two variables. When the speed of the squeegee applied is increased, the shear tension and strain will increase simultaneously.

Two-dimensional (2D) CFD method was used by Rusdi *et al., (*2020) to investigate the flow properties of lead-free and leaded solder pastes [10]. Characterization of solder pastes and rheological studies, together with computational simulations, had been hitherto offer unobtainable insight behind the mechanism of stencil printing process. A three-dimensional (3D) numerical simulation was built by Thankur *et al.*, (2015) to provide an estimate on the amount of solder paste deposited through a stencil [11]. For the purpose of producing the numerical simulation, a combination of Cross viscosity model, as well as Volume of Fluid (VOF) technique, was utilized. The SAC305 type 3 solder paste was utilized, which is a solder paste that is often employed in the industry standard. The experiment and simulation results for solder paste used were noticeably comparable with each other. Different aperture sizes gave comparable outcomes, and results of the experiments are consistent. With CFD technique, research on the impacts of process factors that influence the stencil printing process has also been conducted by Mansur *et al.*, (2020) [12]. In order to complete this experiment, Sn3.5Ag solder paste was utilised. A faster squeegee speed results in higher shear stress values, which in return causes the shear strain rate of the solder paste to increase proportionally. This makes it possible for the solder paste to be applied rapidly and fill the gap. In stencil printing, the uniformity of solder paste filling is critical.

The inclusion of solder paste material features in the simulation model, notably its viscosity attributes, is required for successful execution of the stencil printing process simulation. Solder paste also has several material features, including non-Newtonian fluid, thixotropic fluid, and shear thinning behaviour [13]. Additionally, increased shear tension of the solder paste will result in a decrease in its viscosity. In the past, researchers evaluated and analysed the viscosity of their solder paste sample using a variety of methods, such as evaluating the fluid viscosity using a viscometer. One of the most used methods was the use of a viscometer.

Chen *et al.,* (2022) conducted a study on the Sn–Ag–Cu solder composite to determine its thermal behaviour and mechanical qualities [14]. According to shear tests, the addition of Cu-CNT could enhance the shear strength of solder joints, and the fracture mode of solder junctions changed from mixed fracture to ductile fracture. According to nanoindentation data, the addition of Cu-CNT may improve the mechanical properties of SAC305 solder, as the hardness and modulus of composite solder can be enhanced by increasing Cu-CNT concentration level.

Dusek *et al.,* (2014) developed prediction equations for the height, area, and volume of printed solder paste during the solder paste stencil printing (SPSP) process utilising the response surface approach [15]. Using 30 various combinations of experiment process parameters, the prediction equations linked with the printing parameters and printing quality of the solder paste are derived. Based on the results, it seems that the volume, area, and height of the printed SAC105 solder paste have significant effect on its transfer efficiency.

When investigating SAC305, SAC405, and Sn62Pb36Ag2, Son *et al.*, (2016) employed a 24 mm diameter cone-plate spindle that was tilted at an angle of 1.565° [16]. According to the findings, the amount of time it takes for tests to begin at almost-stored temperatures and terminate at ambient temperatures causes the viscosity of solder pastes to decrease by almost fifty percent.

Roll-offset (RO) printing requires lead-free solder pastes, thus Min-Jung Son and colleagues [17] investigated the distinctions between microparticles and nanoparticles in these pastes. The pastes were designed to use in roll-offset printing. A rotational rheometer with a 1° cone-and-plate arrangement is used for the purpose of assessing the rheological characteristics of SAC solder pastes. This is done with the aid of a revolving rheometer. The cone gap has a diameter of 0.052 mm, and its breadth is 60 mm. A serrated parallel-plate spindle was utilised in Mallik *et al.* [18]'s investigation of the rheological properties for no-clean flux solder. The rheological properties of no-clean flux solder were evaluated alongside those of four other alloy compositions, metal alloys, and particle sizes. Testing was done on solder paste in preparation for the flip-chip assembly. A series of printing evaluations were carried out in order to investigate the nature of the connection that exists between the rheological properties of solder paste and the printed output.

Recent research performed by Rusdi *et al.,* (2019) focusing on analytical process (mathematical modelling) to derive the deformation equation of wedge squeegee with variable section using the semi-inverse method from elastic mechanics [19]. They discovered that the printing angle influences hydrodynamic pressure the most. However, the analytical method has a disadvantage when curves intersect at a certain place. One of the key advantages of CFD over analytical methods is that position of the sudden rise in hydrodynamic pressure is slightly divergent in CFD, whereas the theoretical curve shows a large departure.

In order for CFD models to be accurate, rheological data must be included in the solder paste's material characteristics. Information on the solder paste's viscosity is necessary to guarantee that the CFD simulation will accurately forecast its flow. Because previous researchers used a wide variety of testing methods, choosing the spindle type that is most suitable for measuring solder paste is quite important. The purpose of this study was to investigate the influence of different spindle type had on CFD simulations. The CFD model will have a number of different viscosity data input in order to identify which viscosity data will provide the most accurate predictions of the filled volume when using CFD. The results of the CFD simulation will be compared to the data that was obtained through experiments. On the SMT line at Celestica Malaysia, a 3D scanner was used to measure the volume of solder paste deposition, and an industrial stencil printing equipment was used to obtain the experimental results. The researcher will benefit from this study's analysis since it will help them choose the viscosity test that is most suited for CFD modelling. In addition, every single piece of experimental work is performed using a genuine SMT machine. In light of the growing need for ecologically safe components, this investigation will make use of SAC305, a solder paste that does not include lead and is utilised to a significant degree by both manufacturers and researchers. Stannum, silver, and copper are the key components utilised in the production of solder paste. Table 1 shows the previous work on solder joints.

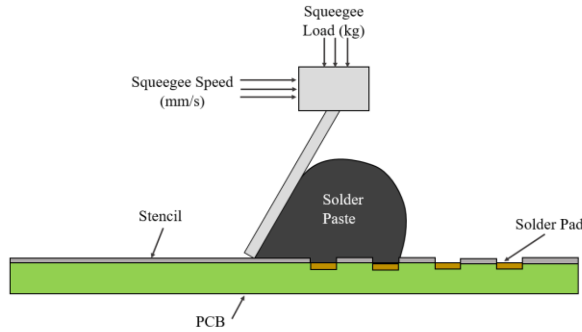

Figure 1 Solder Paste Stencil Printing Process

Table 1 Previous work on solder joints

Authors	Results and findings
Hirman *et al.* [6]	Optimization of solder paste, and the desired parameter of the soldered joint is investigated by experiment. They found that decreasing the amount of solder paste by 74% will caused 10% loss in mechanical shear strength.
Khader *et al.* [7]	Developed a novel mixed-integer nonlinear programming (MINLP) model with the intention of enhancing the printing settings for a variety of PCB pad layouts. The results show that MINLP is capable of effectively solving problems with specification limits ranging from 50 to 150 %, 70 to 130 %, and 80 to 120 %.
Chen *et al.* [14]	The shear fracture behaviors of composite solder joints and the development of interfacial intermetallic compounds (IMCs) were studied. Using Cu-CNT as the reinforcing phase of SAC305 solder may slow the growth of IMC, as shown by the data.
Chen *et al.* [15]	Utilizing response surface methods, the dependency of process factors influence on printing quality is investigated. According to the test data, if the desired solder paste height is 100 µm, the ideal printing parameters are 175.08 N printing pressure, 250 mm/s printing speed, 0.1 mm snap-off height, and 15.7 mm/s stencil snap-off speed.

2.0 METHODOLOGY

2.1 Viscosity Test

The viscosity of solder paste was measured using an Anton Parr viscometer (Figure 2). Three different kinds of spindles (1.014° Cone Plate, 2° Cone Plate, and Parallel Plate) were used in this study. While the 1.014° Cone plate and the 2° Cone plate's gap heights were kept at their original values, they were changed for Parallel Plate's (Table 2). It was calculated by measuring the distance between fixed and spindle plates and determining the height of the gap (below and top). The spindle will rotate at a specified speed while the bottom plate remains stationary to retain control over the shear rate. The shear rates employed in the experiment ranged from 0.001 s^{-1} all the way up to 10 s^{-1} [12]. All viscosity tests were performed at room temperature (25.2° Celsius). As seen in Figure 3, a Cone Plate spindle differs significantly from a Parallel Plate spindle. Data on viscosity and shear rate are then entered into WinRheo, which calculates values for Cross' model based on this information. For the purpose of this experiment, the SAC305 was selected since it is the lead-free solder paste that is most commonly used in the industry. Indium Corporation was the supplier for the solder paste used.

Figure 2 Anton Parr Viscometer and Spindle

Table 2 Spindle size and gap height

Spindle	Diameter (mm)	Gap Height (mm)
Cone Plate 1.014°	24.980	0.051
Cone Plate 2.008°	24.981	0.104
Parallel Plate Gap A	24.985	0.250
Parallel Plate Gap B	24.985	0.500
Parallel Plate Gap C	24.985	0.750

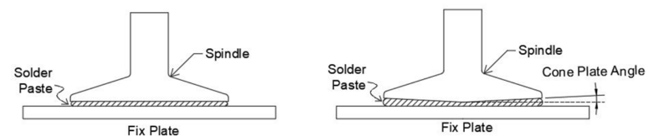

Figure 3 Rheology test schematic diagram

2.2 Stencil Printing Process Experiment

An industrial solder paste printing machine was used to perform experiments while it was in operation. The angle of squeegee is set at a constant angle of 60° and moved at 35 mm/s [20]. An 9 kg load, 35 mm/s squeegee was used. After that, the dimensions of the solder pastes were measured using a Koh Young Aspire 2 3D scanner. The stencil printing tests were carried out at Celestica Malaysia with a temperature

of (25.2 ° C.), which was considered to be the room temperature. The angle of the squeegee was adjusted to be 60 °, and a stainless-steel stencil with the following dimensions: 730 mm by 735 mm and a thickness of 0.127 mm was used.

2.3 Numerical Simulation

Version 19 of ANSYS Fluent programme is utilized for the numerical simulations that are required for this study. ANSYS Fluent is a reliable piece of CFD software that, by employing the Finite Volume Method, can provide a realistic simulation of the stencil printing process. In this investigation, the Navier–Stokes method was applied to calculate and investigate the process of SAC305 solder paste being fed into the stencil aperture by utilizing conservation of mass, momentum, and energy as the governing equations. This was done by applying the Navier–Stokes method to the data obtained from the experiment.
The conservation of mass or continuity equation is:

$$\frac{\partial u}{\partial x}+\frac{\partial v}{\partial y}+\frac{\partial w}{\partial z}=0 \quad (2.1)$$

Equation (2.1) is the mass conservation equation in which it is valid for incompressible flow. The Conservation of momentum equation in x-, *y*- and z-direction is written as:

$$\rho\left(\frac{\partial u}{\partial t}+u\frac{\partial u}{\partial x}+v\frac{\partial u}{\partial y}+w\frac{\partial u}{\partial z}\right)=-\frac{\partial P}{\partial x}+\eta\left(\frac{\partial^2 u}{\partial x^2}+\frac{\partial^2 u}{\partial y^2}+\frac{\partial^2 u}{\partial z^2}\right) \quad (2.2)$$

$$\rho\left(\frac{\partial v}{\partial t}+u\frac{\partial v}{\partial x}+v\frac{\partial v}{\partial y}+w\frac{\partial v}{\partial z}\right)=-\frac{\partial P}{\partial y}+\eta\left(\frac{\partial^2 v}{\partial x^2}+\frac{\partial^2 v}{\partial y^2}+\frac{\partial^2 v}{\partial z^2}\right) \quad (2.3)$$

$$\rho\left(\frac{\partial w}{\partial t}+u\frac{\partial w}{\partial x}+v\frac{\partial w}{\partial y}+w\frac{\partial w}{\partial z}\right)=-\frac{\partial P}{\partial z}+\eta\left(\frac{\partial^2 w}{\partial x^2}+\frac{\partial^2 w}{\partial y^2}+\frac{\partial^2 w}{\partial z^2}\right) \quad (2.4)$$

where *P* is the static pressure, ρ is density, η is the viscosity and u, v, w is the velocity in x-, *y*- and z-direction. The conservation energy equation can be described as:

$$\rho c_p\left(u\frac{\partial T}{\partial x}+v\frac{\partial T}{\partial y}+w\frac{\partial T}{\partial z}\right)=k\left(\frac{\partial^2 T}{\partial x^2}+\frac{\partial^2 T}{\partial y^2}+\frac{\partial^2 T}{\partial z^2}\right)+\eta\dot{\gamma} \quad (2.5)$$

where k is the thermal conductivity, T is the temperature, η is the viscosity and $\dot{\gamma}$ is the shear rate. In order to analyse the rheological behaviour of the solder paste, the Cross-model viscosity model [21] was utilised. When the Cross model is used as the viscosity model, the solder paste is considered to be GNF with an Arrhenius temperature dependency, and this assumption is used;

$$\eta(T,\dot{\gamma})=\frac{\eta_0(T)}{1+\left(\frac{\eta_0\dot{\gamma}}{\tau^*}\right)^{1-n}} \quad (2.6)$$

with

$$\eta_0(T)=B\exp\left(\frac{T_b}{T}\right) \quad (2.7)$$

where B is an Exponential-fitted constant, T_b is the temperature-fitted constant, η is described as the power law index, η_0 is designated as the zero-shear viscosity and τ^* refer to a parameter that explain the transition region that exist between power law region of the solder paste viscosity curve and the zero-shear rate.

By giving a scalar value to each cell in the computational grid, the VOF method was able to locate the existence of liquid phase and determine its distribution (f). The amount of space within the cell that is taken up by liquid is represented by the symbol f. Therefore, f equals 1 (f = 1) when the cell is only filled with solder paste, whereas f equals 0 (f = 0) when the cell is only filled with air, and when f is between 0 and 1, it is solder paste front (interface cells). The equation used to describe the progression of the melt front over time is as follows:

$$\frac{dF}{dt}=\frac{\partial F}{\partial t}+\nabla\cdot(uf)=0 \quad (2.8)$$

Using VOF, the simulation characterised air and solder paste as two distinct fluid phases that were independent from one another. The squeegee was shown as a moving wall, and it was moving at a predetermined pace while utilising a dynamic mesh. As the squeegee is moved, the solder paste will travel forward and fill the aperture as it does so. In the interim, the air will be allowed to leave the building through the various vents. During the FLUENT study, the computational domain was utilised to determine the boundaries of the moving wall bounds, the pressure outlet, and the symmetry walls. The boundary conditions for the 3D simulation model are depicted in Figure 4.

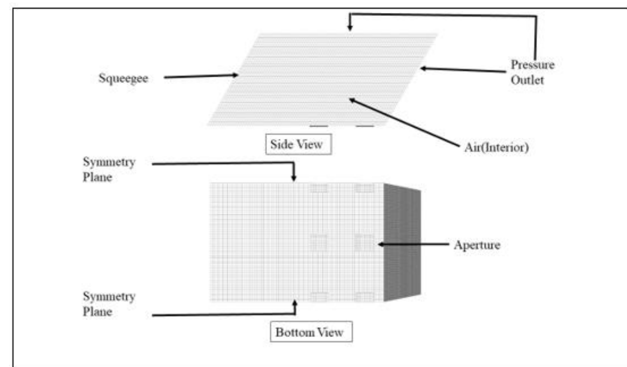

Figure 4 Mesh and Boundary conditions

2.4 Grid Independence and Time Step Test

In the process of numerical simulation analysis, the time step size and grid size are extremely important factors to consider since they have the potential to either exaggerate or underestimate the outcomes of the experiment. It was determined that the best simulation predictions could be made using 2632 hexagonal components and five different time-step sizes (0.01, 0.005, 0.001, 0.0005, and 0.0001). A squeegee load of 9 kg was used, with a squeegee speed of 35 mm/s and a separation speed of 0.03 mm/s used for the tests, which represent real life situations. In order to validate the results, the volume of solder paste used in both the numerical prediction and the experiment was measured and compared. The results are presented in Table 3. According to the findings, every numerical simulation result produced an inflated estimate for the amount of solder paste used. The error rate reached 7.4% when 0.001-time step size was utilized for Case 3. As a direct result of this, Case 3 with a time step size of 0.001 was selected for further investigation due to the fact that it had the lowest error when measured against the trial outcomes. Example 3's experimental measurements and simulation results are depicted in Figure 5,

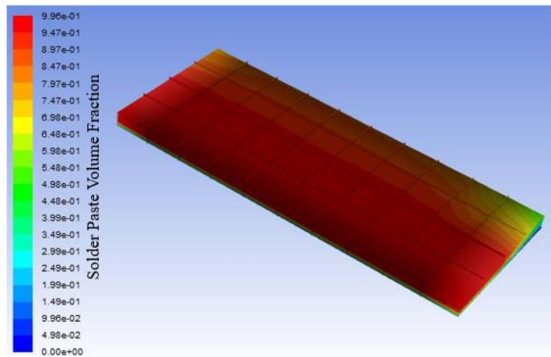

Simulation

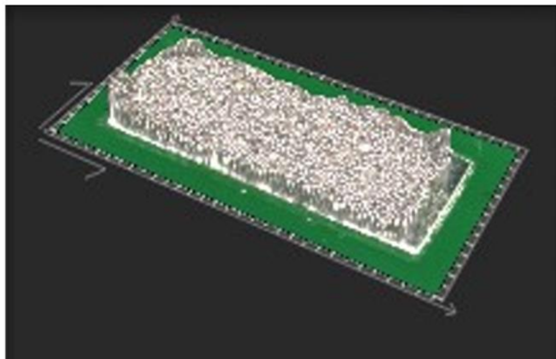

Experiment

Figure 5 Solder paste measurement using Koh Young 3D scanner and CFD simulation result for 1210 Resistor (2.54 mm × 1.016 mm)

In order to conduct the grid independence test, five distinct hexagonal mesh pieces were first constructed. The findings of the simulation were compared to the volume of solder paste that was found to be in the aperture after carrying out the experiment. The outcomes of the comparison between the experimental results and simulation data are tabulated and summarised in Table 4. Case 2, which has a total of 2632 elements, has the least significant error, followed by Case 3, which has 3712 elements, and Case 5, which has 7072 elements. A computational domain with 2632 elements and a time step of 0.001 was chosen for further investigation and analysis based on the results of the time step and grid independency tests.

Table 3 Time Step study

Case	1	2	3	4	5	
Time step	0.01	0.005	0.001	0.0005	0.0001	Experiment
Solder Volume (m^3)	0.7008324	0.7077731	0.713686	0.7115767	0.6425067	0.770773118
Error (%)	9.1	8.2	7.4	7.7	16.6	-

Table 4 Grid Independence Study

Case	1	2	3	4	5	
No. Of Elements	1952	2632	3712	5192	7072	Experiment
Solder Volume (m^3)	0.6856809	0.713686	0.7115409	0.7084583	0.7103076	0.770773118
Error (%)	11.0	7.4	7.7	8.1	7.8	-

3.0 RESULTS AND DISCUSSION

3.1 Effect of Different Spindle for Measuring

A total of five spindle tests were carried out, each of which utilised a different type of spindle than the previous test (Figure 6). For PP, the plate gaps were set at 0.25 mm, 0.5 mm, and 0.75 mm. Two different CP spindles were used, one at an angle of 1°, and the other at an angle of 2°. In contrast to the results of the other tests, the viscosity value of 1° CP is the highest. Throughout the whole shear rate range, 0.25 mm PP and 0.5 mm PP produce values of viscosity that are almost identical to one another. On the other hand, the viscosity values of 2° CP and 0.75 mm PP are comparable to one another. The 1° CP is anticipated to have the highest viscosity values due to the fact that its plate gap is the smallest, at 0.051 mm. The 0.25 mm PP and 0.5 mm PP spindles are both of the same type, with just a little variation in distance between the spacing. For 2° CP, the gap with lowest measurement of 0.104 mm has the same viscosity as the gap with broadest measurement of 0.75 mm in PP. A narrow space of 0.104 mm is found to exist between the point of the cone and the connecting plate. The distance between the spindle and the end cap is 0.453 mm. It is speculated that this is due to the fact that wider gaps have less axial

tension, which in return leads to lower viscosity values in tests done using larger gap spindles.

3.2 Effect of Different Squeegee Speed

The results of spindle tests and the experiment with different squeegee speeds are compared to one another. Figure 7 illustrates the volume of aperture filling that occurs with solder paste when different squeegee speeds are used. The results of experiment was underestimated by the simulation outcome as shown in Figure 7. Only 0.5 mm PP and 2° CP display a pattern equivalent to the other two, with the exception of 55 mm/s, when 0.5 mm PP achieve the same outcome as its 45 mm/s value. A further in-depth examination of 2° CP obtained a value that was somewhat lower than the 45 mm/s figure.

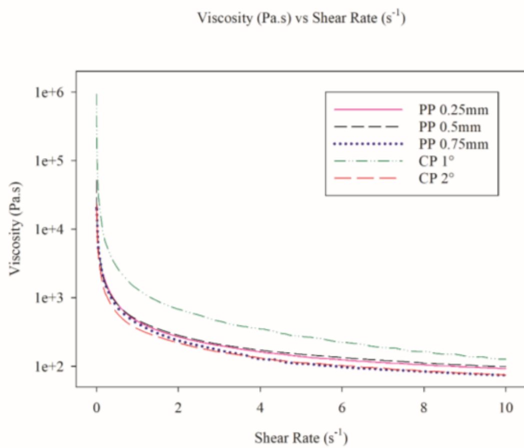

Figure 6 Viscosity versus shear rate at different spindle test.

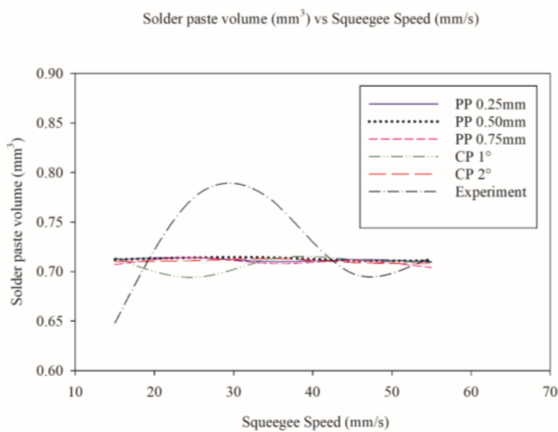

Figure 7 Solder paste volume at different squeegee speed

Figure 8 illustrates the percentage difference between the volume of solder paste used in simulation and experiment. It is observed that among the various squeegee speeds, the 0.5 mm PP has the lowest average difference at 5.4 %, whilst the 1° CP has the biggest average discrepancy at 6.1 %. Other tests have reported findings that are comparable to these, with the exception of 1° CP experiment, which shows the difference was largest at 25 mm/s. Nevertheless, at the point of fluctuation with the least amount of variance, 55 mm/s, all of the experiments had the same findings. When the speed of the squeegee rises, there may be a corresponding reduction in viscosity of the liquid. The obtained findings were consistent with Figure 6, which shows that the viscosity value for all of the spindle tests become more comparable as the shear rate increases (i.e., as the speed of the spindle increases).

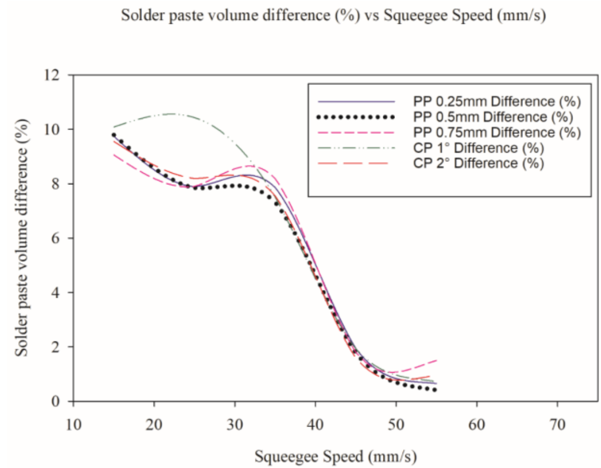

Figure 8 Solder pastes volume difference in percentage at different squeegee speed

3.3 Effect of Different Aperture Size

Figure 9 depicts the results of calculating the aperture size for each of the three different aperture volumes (0.09 mm^3, 0.33 mm^3 and 0.82 mm^3). All spindle tests use the same squeegee speed, which is set at 35 mm/s. According to figure 9, consistent patterns can been seen in all of the tests since the experiment and volume of the values obtained from all of the tests are comparable. This identical pattern was also largely consistent with Figure 8, which demonstrates that the spindle test values are very close to one another when the squeegee is moving at 35 mm/s. The volume of solder pastes rose as well when compared to the aperture volume, which went from 0.1 mm^3 to 0.8 mm^3 in size. At smaller aperture volumes, the difference between the experimental and simulated values is miniscule. As the aperture volume rises, the discrepancy becomes more apparent. With reference to Figure 10, it can be seen that the volume percent difference of solder paste reduces in a progressive manner as the aperture volume grows. The difference in percentage terms that is the least possible between 0.5 mm PP and 1° CP is 11.6%. When the aperture volume decreased, the volume of solder paste produced by tests varying viscosity values results in approximately the same volume of solder paste (as depicted in Figure 11). The 0.5 mm PP viscosity test produces improved findings

with lower volume difference compared to other viscosity tests when the aperture volume is increased.

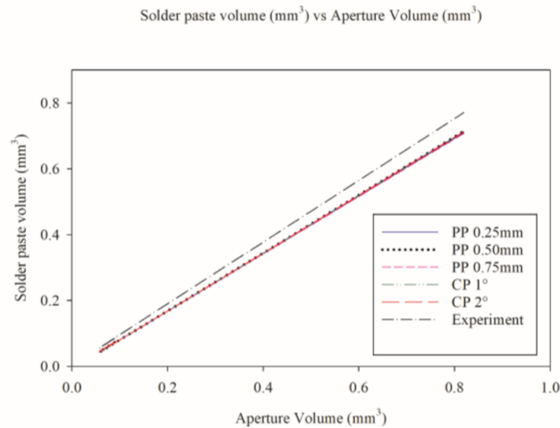

Figure 9 Solder paste volume at different aperture size

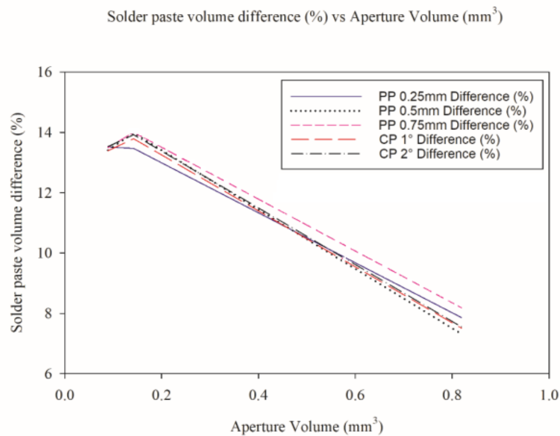

Figure 10 Solder pastes volume difference in percentage at different aperture size

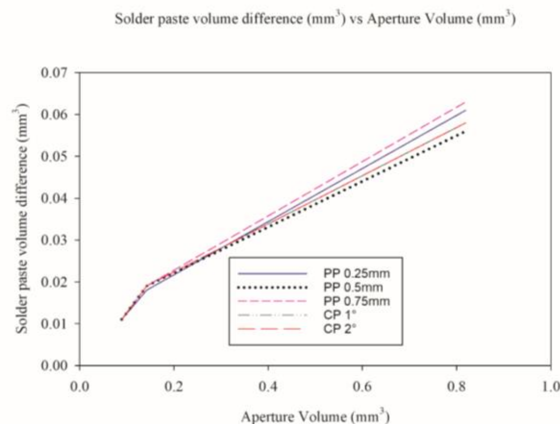

Figure 11 Solder pastes volume difference at different aperture size

4.0 CONCLUSION

In each of the five different tests performed, both PP and CP type spindles were successfully investigated. Plate spacing was varied between 0.25 mm and 0.75 mm for PP, with 0.5 mm being the most common. The CP was made up of two plate angles, one measured at 1° and the other by 2°. The results of all five viscosity tests were compared in order to find out which one was the most accurate for CFD simulations. In order to evaluate the practicability of the model, a grid independence test was carried out. Following this, data comparison between the simulation and the experiment results was carried out. The results showed that the CFD simulation matched the experimental trends by an average of 7.8 %. The CFD simulation model and the actual work were analysed and contrasted in a number of different ways at a number of different squeegee speeds and aperture size modifications. The PP with 0.5 mm gap produces the least average difference between simulation and experiment, which comes in at 5.4 %. This is the case regardless of squeegee speed setting used. The smallest average disagreement, 11.6 %, was found at 1° CP and PP with 0.5 mm gap, although the trend and average difference were comparable across all aperture sizes. Similar patterns were observed in each test at smaller aperture volumes, however at larger aperture volumes, 0.5 mm PP showed the least % deviation from experimental values. This was due to the fact that it had the smallest aperture volume. The effect of different viscometer tests for addition of nanoparticle in lead-free solder material can be further investigated as well. The addition of nanoparticles usually focuses on the strength and reliability of the solder joint only.

Acknowledgement

The authors would like to express their gratitude to the Short-Term Research Grant, Universiti Sains Malaysia (304/PMEKANIK/6315569) for their financial assistance. As well as the School of Mechanical Engineering, Universiti Sains Malaysia and Celestica Malaysia Sdn. Bhd. for simulation and experimental works conducted at their facilities.

References

[1] Illés, B., Krammer, O., and Géczy, A. 2020. Chapter 1 - Introduction to Surface-Mount Technology. *Reflow Soldering*. 1-62.
DOI: https://doi.org/https://doi.org/10.1016/B978-0-12-818505-6.00001-7

[2] Tsai, T. N., and Liukkonen, M. 2016. Robust Parameter Design for The Micro-BGA Stencil Printing Process Using a Fuzzy Logic-Based Taguchi Method. *Applied Soft Computing Journal.* 48: 124-136.
DOI: https://doi.org/10.1016/j.asoc.2016.06.020.

[3] Huang, C. Y. 2018. Applying the Taguchi Parametric Design to Optimize the Solder Paste Printing Process and the Quality Loss Function to Define the Specifications. *Soldering and Surface Mount Technology*. 30(4): 217-226.
DOI: https://doi.org/10.1108/SSMT-03-2017-0010.

[4] Geczy, A., Hajdu, I., Gal, L., Barna, C. N., Kovacs, M., and Harsanyi, G. 2019. Challenges of SMT Assembling on Biodegradable PCB Substrates. *22nd European Microelectronics and Packaging Conference & Exhibition (EMPC)*. 1-5.
DOI: https://doi.org/10.23919/EMPC44848.2019.8951848.

[5] Hirman, M., and Steiner, F. 2017. Optimization of Solder Paste Quantity Considering the Properties of Solder Joints. *Soldering & Surface Mount Technology*. 29(1): 15-22.
DOI: https://doi.org/10.1108/SSMT-10-2016-0025.

[6] Khader, N., and Yoon, S. W. 2018. Stencil Printing Process Optimization to Control Solder Paste Volume Transfer Efficiency. *IEEE Transactions on Components, Packaging and Manufacturing Technology*. 8(9): 1686-1694.
DOI: https://doi.org/10.1109/TCPMT.2018.2830391.

[7] Krammer, O. 2014. Finite Volume Modelling of Stencil Printing Process. *IEEE 20th International Symposium for Design and Technology in Electronic Packaging, SIITME*. 79-82.
DOI: https://doi.org/10.1109/SIITME.2014.6966998.

[8] Manessis, D., Patzelt, R., Ostmann, A., Aschenbrenner, R., and Reichl, H. 2004. Technical Challenges of Stencil Printing Technology for Ultra Fine Pitch Flip Chip Bumping. *Microelectronics Reliability*. 44(5): 797-803.
DOI: https://doi.org/10.1016/S0026-2714(03)00361-5.

[9] Durairaj, R., Jackson, G. J., Ekere, N. N., Glinski, G., and Bailey, C. 2002. Correlation of Solder Paste Rheology with Computational Simulations of the Stencil Printing Process. *Soldering and Surface Mount Technology* 14(1): 11-17.
DOI: https://doi.orget a/10.1108/09540910210416422.

[10] Rusdi, M. S., Abdullah, M. Z., Ishak, M. H. H., Abdul Aziz, M. S., Abdullah, M. K., Rethinasamy, P., and Jalar, A. 2020. Three-Dimensional CFD Simulation of the Stencil Printing Performance of Solder Paste. *The International Journal of Advanced Manufacturing Technology*. 108(9-10): 3351-3359.
DOI: https://doi.org/10.1007/s00170-020-05636-9.

[11] Thakur, V., Mallik, S., and Vuppala, V. 2015. CFD Simulation of Solder Paste Flow and Deformation Behaviours during Stencil Printing Process. *International Journal of Recent Advances in Mechanical Engineering*. 4(1): 1-13.
DOI: https://doi.org/10.14810/ijmech.2015.4101.

[12] Mansor, Nur Hidayah, Mohd Sharizal Abdul Aziz, Nina Amanina Marji, and Mohd Arif Anuar Mohd Salleh. 2020. Effect of Temperature on Solder Paste During Surface Mount Technology Printing. *Journal of Advanced Research in Fluid Mechanics and Thermal Sciences*. 75. Penerbit Akademia Baru. 3: 99-107.
DOI: https://doi.org/10.37934/arfmts.75.3.99107.

[13] Chen, B., Wang, H., Zou, M., Hu, X., Chen, W., and Jiang, X. 2022. Evolution of Interfacial IMCs and Mechanical Properties of Sn–Ag–Cu Solder Joints with Cu-modified Carbon Nanotube. *Journal of Materials Science: Materials in Electronics*. 33: 19160-19173.
DOI: https://doi.org/10.1007/s10854-022-08753-1.

[14] Chen, C. H., Wang, H., Kao, Y. C., Lu, P. J., and Chen, W. R. 2022. Predictive Model of the Solder Paste Stencil Printing Process by Response Surface Methodology. *Soldering & Surface Mount Technology*.
DOI: https://doi.org/10.1108/SSMT-08-2021-0056.

[15] Dusek, K., Pelikanova, I. B., Busek, D. and Zeidler, M. 2014. Measurements of Solder Paste Viscosity During Its Tempering and Aging. *Proceedings of the 37th International Spring Seminar on Electronics Technology*. 189-192.
DOI: https://doi.org/10.1109/ISSE.2014.6887590.

[16] Son, M. J., Kim, I., Yang, S., Lee, T. M. and Lee, H. J. 2016. Employment of Roll-Offset Printing for Fabrication of Solder Bump Arrays: Harnessing the Rheological Properties of Lead-Free Solder Pastes Using Particle Size Distribution. *Microelectronic Engineering*. 164: 128-134.
DOI: https://doi.org/10.1016/j.mee.2016.07.012.

[17] Mallik, S., Schmidt, M., Bauer, R., and Ekere, N. N. 2010. Evaluating Solder Paste Behaviours Through Rheological Test Methods and Their Correlation to the Printing Performance. *Soldering and Surface Mount Technology*. 22(4): 42-49.
DOI: https://doi.org/10.1108/09540911011076871.

[18] Liu, Y., Meng Z., Ji, C., and Chen, Y. 2022. Mathematical Modelling of Flow Field In 3-Dimensional Additive Printing. *International Journal of Mechanical Sciences*. 224: 107326.
DOI:https://doi.org/https://doi.org/10.1016/j.ijmecsci.2022.107326.

[19] Rusdi, M. S., Abdullah, M. Z., Chellvarajoo, S., Abdul Aziz, M.S., Abdullah, M. K., Rethinasamy, P., Veerasamy,S., and Santhanasamy, D. G. 2019. Stencil Printing Process Performance on Various Aperture Size and Optimization for Lead-Free Solder Paste. *The International Journal of Advanced Manufacturing Technology 102. The International Journal of Advanced Manufacturing Technology*. (9-12): 3369-3379.
DOI:https://doi.org/https://doi.org/10.1007/s00170-019-03423-9.

[20] Rusdi, M. S., Abdullah, M.Z., Aziz, M. S. A., Abdullah, M. K., Ishak, M. H. H., Hwa, Y. K., Rethinasamy, P., Veerasamy, S., and Santhanasamy, D. G. 2019. SAC105 Stencil Printing Process Using Cross Viscosity Model. *Journal of Advanced Research in Fluid Mechanics and Thermal Sciences*. 54(1): 70-77.